Visualization and image processing of spray structure under the effect of cavitation phenomenon

M Ghorbani[(1)], G Alcan[(1)], D Yilmaz[(2)], M Unel[(1)], A Kosar[(1)*]

[(1)]Mechatronics Engineering Program, Faculty of Engineering and Natural Sciences, Sabancı University, Orhanlı, Tuzla, Istanbul, Turkey
[(2)]Manufacturing Systems Program, Faculty of Engineering and Natural Sciences, Sabancı University, Orhanlı, Tuzla, Istanbul, Turkey

Abstract. This paper presents visualization and image processing of spray structure affected by cavitation bubbles and cavitating flow patterns. Experiments were conducted for a better understanding of cavitation and resulting flow regimes. Cavitation is generated with sudden pressure drop across a 4.5 *mm* long short micro-channel with an inner diameter of 152 μm connected to the setup using proper fittings. Generated cavitation bubbles and fluid flow patterns were observed by using a high speed camera. The spray structure was observed in four different segments and mainly the droplet evaluation in the lower segments for low upstream pressures was analyzed using several image processing techniques including contrast adjustments and morphological operators. Moreover, fluid flow regimes for different upstream pressures were investigated, and the flow patterns were analyzed in the separated regions of the spray.

1. Introduction

One of the most significant parameters affecting spray characteristics is cavitation with cavitation bubbles inside an orifice, which may extend to the outlet and impact the spray via bubble collapse. The cavitation bubbles and cavitating flow patterns were recently experimentally visualized in transparent nozzles [1-3]. Payri et al. [4] visualized existing cavitation bubbles at the outlet of the orifice using the special near-nozzle field visualization technique with the aid of a test rig pressurized with fuel. They attempted to investigate the effect of the nozzle geometry on cavitation patterns and the spray formation. They showed that cavitation inception and chocked flow conditions differed in terms of the pressure values, and also, the spray cone angle increased with cavitation. The flow regimes under cavitating flow conditions were studied by looking at the variations in the frequency of the cavitation shedding in the internal nozzles [5] and by analyzing the periodic shedding of the cavitation phenomenon using high speed cameras [6]. In this regard, De Giorgy et al. [7] studied flow regimes under the effect of cavitation phenomenon using a CCD camera and presented an analysis on pressure fluctuation frequency. Their experimental observations illustrated different flow regime maps (from inception to cavitating jets) under various working conditions.

In this study, the spray structure was visualized using a high speed imaging system in order to detect the details of the fluid flow regime and droplet discretization at the end of the spray. Acquired images were enhanced using several image processing algorithms such as contrast adjustment, morphological operators and connected component analysis (CCA). Enhanced images provide better visualization of bubbles and enable analysis of bubbles.

2. Experimental Setup and Procedure

2.1. Hydrodynamic Cavitation

A schematic of the experimental setup is shown in Figure 1. The experimental setup consists of a high pressure pure nitrogen tank (Linde Gas, Gebze, Kocaeli), a liquid container (Swagelok, Erbusco BS, Italy), pressure sensors (Omega, USA.), fine control valves (Swagelok) at different locations, a micro

* To whom any correspondence should be addressed. Email: kosara@sabanciuniv.edu

filter (Swagelok), a turbinemeter (Omega, USA), a Phantom high speed camera (Phantom V320 high speed camera) with appropriate lenses, a workstation with visualization software (Phantom PCC 2.0 software), fittings (Swagelok), and microchannel (Small Parts, USA.) connected to the setup with appropriate fittings for cavitation formation. The tank was used as a container for de ionized (DI) water and high pressure nitrogen tank was connected to the liquid container in order to maintain high input pressure and propel the fluid to the microprobe. During the experiments, valves were fully opened and cavitation is generated with sudden pressure drop across a 4.5 *mm* long short microchannel with an inner diameter of 152 *μm* connected to the setup using proper fittings.

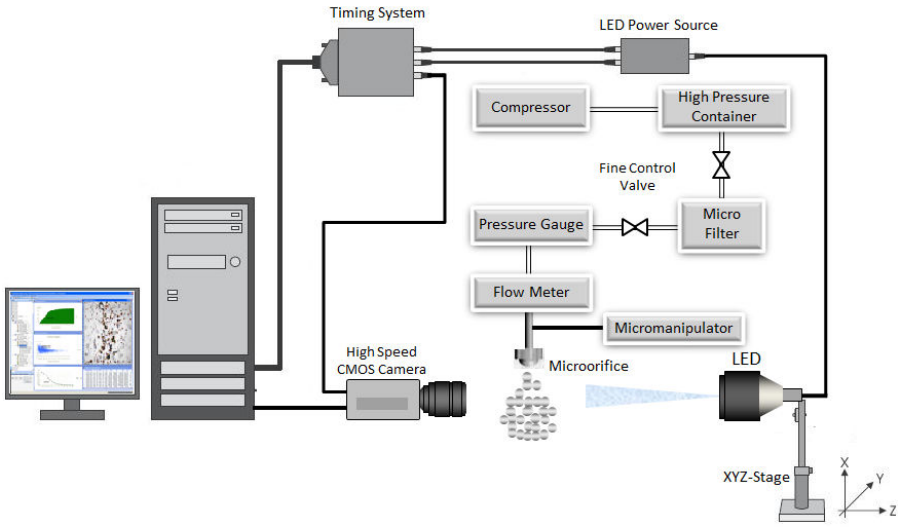

Figure 1. Experimental setup configuration with the orifice throat and exit area

2.2. Experimental Procedure

Experiments were conducted by adjusting the inlet pressures. Inlet pressures were varied from 10 *bars* to 120 *bars*, while outlet pressure at the microchannel was fixed to 1 *atm*. Volumetric flow rate was increased with the change in the inlet pressure. At a certain pressure level, cavitation inception was observed with the high speed camera. Bubbly cavitating flows generated in the microchannel was recorded at different regions (four segments, at distances of 0-3.5, 3.5-7.3, 7.3-11.1 and 11.1-14.9 *mm* from the microchannel outlet) downstream the microchannel outlet.

3. Results and Discussion

Emerging flow patterns from the micro orifice exit are displayed in Figure 2 in various segments for a constant upstream pressure of 30 *bars*. The variation in cavitation number is shown in Figure 3, which presents the effect of the upstream pressure on the spray shape. Cavitation number at lower injection pressures starts from 1.37 and decreases to 0.1108 at P_i= 110 *bars* (P_i is upstream pressure) for segment 1, which indicates a highly vaporous cavitation pattern for higher upstream pressures. X/D indicates the ratio of the spray length with respect to the diameter of the microchannel. As shown in Figure 3, a highly vaporous bubbly flow is observed at cavitation numbers below 0.4, which corresponds to upstream pressures more than 80 *bars* in all segments and the first segment of the upstream pressure of 50 *bars*. Bubbly flow is visualized between cavitation numbers of approximately 0.8 and 0.4. Upstream pressures of 50 *bars* for all the segments and the first segment of 30 *bars* generate bubbly flow at the outlet of the microchannel. Jet cavitation is observed below the cavitation number of 1, which indicates the effect of generated cavitation bubbles inside the microchannel on the structure of the spray. Above this number, the spray contains just single liquid jet affected by the throat velocity. Above the cavitation number of 2, the droplets begin to appear and continuous flow changes to discrete droplet flow, which is shown in the third and fourth segments for the cases corresponding to upstream pressures below 20 *bars*.

Before starting with the analysis of droplets in these segments, images need to be processed and purified from the noise to detect droplets in a correct way. Since high speed CMOS camera provides 8-bit grey-scale images, droplets could not be distinguished from background easily due to shadows, noise and undesired particles in unprocessed original images (Figure 4 (a)).

Figure 2. Bubble cloud emerging that is captured through increasing distance from the probe exit, respectively (P_i=30 *bars*)

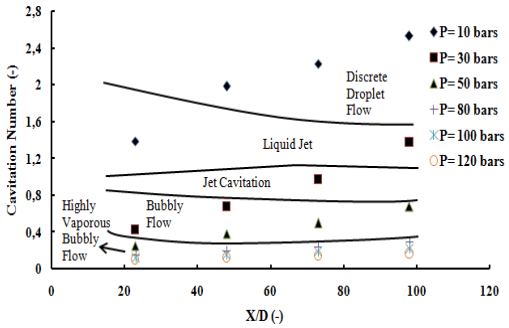

Figure 3. Cavitation number for different upstream pressure in various locations along the spray

Increasing the contrast of the images is the first step of visual processing. Image adjustment allows 1% of data to be saturated at low and high intensities of the image. This increases the contrast of the image and makes foreground distinguishable from background (Figure 4(b)). Histogram equalization enhances the contrast by transforming the values of the image, in the colormap of indexed image. It is generally applied to images with very close histogram values. To eliminate the noise which is generated by histogram equalization and to get smoother images, 'morphological opening' operation is applied (Figure 4(c)). Morphological opening is the dilation of the erosion of the image by a structuring element. In this case, structuring element was chosen as a 3x13 vertical rectangle because droplets were like rectangles, not circles. Morphological opening was the final step of noise removal process and purified images were thresholded by Otsu's method [8] to segment the droplet candidate regions. Finally binary images were formed to investigate the regions by Connected Component Analysis (CCA). CCA looks for the relationships between pixels, divides them into different groups and labels. In each group, pixels were located in the neighbourhood of each other. All labelled regions in processed binary images were candidates of droplets (Figure 4 (d)).

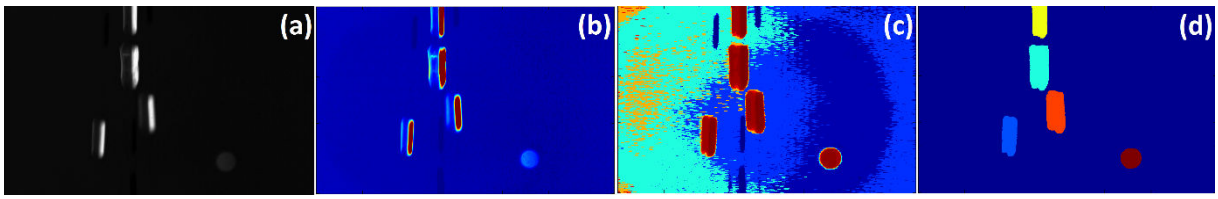

Figure 4. Image processing steps **(a)** Original raw image **(b)** Contrast adjustment **(c)** Histogram equalization and morphological opening **(d)** Connected component analysis (P_i=10 *bars*)

Until now, processing may not completely clean the noises. To eliminate the noise regions, region properties were utilized. Clearly, droplets have some considerable amount of pixel-wise area between 5000 and 15000. Thus, regions with less than a certain pixel-wise area can be treated as noise and were excluded. Apart from these areas, there were some circular regions which did not flow like other droplets. The shape of droplet was utilized in this case to get rid of circular noise (Figure 5). In geometry, eccentricity of a shape represents how close it is to a pure circle. This number is between 0 - 1 and it is close to 1 if the shape is pure circle. Obviously eccentricities of droplets and circular noises are far from each other.

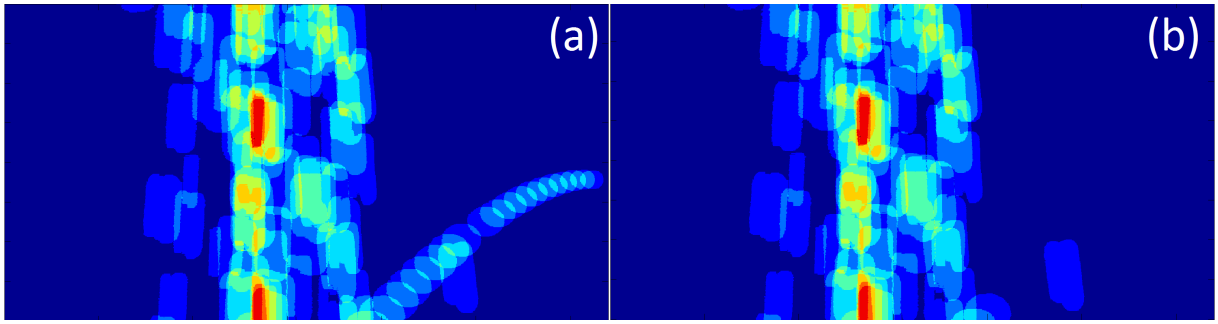

Figure 5. (a) Existence of circular noise **(b)** Removal of circular noise (P_i=10 *bars*)

In addition to discrete droplets visualization, scattered bubbles around jet spray were also determined by the same image processing method with a slight modification. After noise removal process steps were applied, CCA algorithm releases information about the properties of scattered bubbles. Figure 6 depicts the frequency of scattered bubbles in different segments of spray structure.

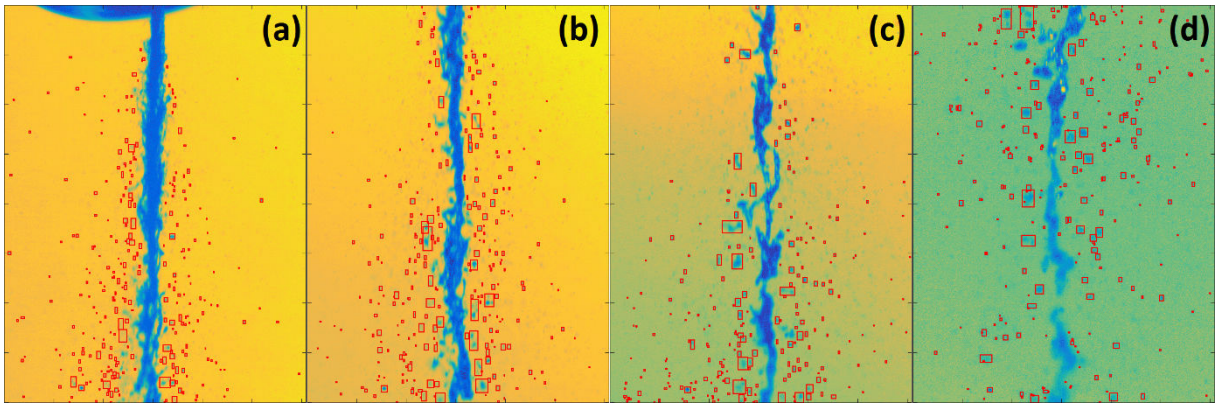

Figure 6. Spray Structure **(a)** Segment 1 **(b)** Segment 2 **(c)** Segment 3 **(d)** Segment 4 (P_i=80 *bars*)

Conclusion

Results show that there are different fluid flow regimes while the upstream pressure varies from 10 to 120 *bars*. Discrete droplet flow, liquid jet, cavitation jet, bubbly flow and highly vaporous bubbly flow were reported as the flow patterns for different cavitation numbers. Highly vaporous bubbly flow is observed at the outlet of the microchannel in the first segment due to very low cavitation number while the upstream pressure was more than 100 *bars*. Moreover, image processing methods were utilized to segment the discrete droplets accurately. Additionally, scattered bubbles around main flow were extracted.

4. References

[1] Andriotis A, Gavaises M, Arcoumanis C, 2008 *J. Fluid Mech.* **610** 195
[2] Suh H K, Lee CS, 2008 *I. J. Heat Fluid Flow* **29** 1001
[3] Mishra C, Peles Y, 2005 *Physics fluids* **17** 013601
[4] Payri R, Salvador F J, Gimeno J, De La Morena J, 2009 *I. J. Heat Fluid Flow* **30** 768
[5] Chandra B W, Collicott S H, 1999 In: 12th Annual Conference ILASS, Americas, 379
[6] Sato K, Saito Y, 2002 *JSME I. J. Ser. B Fluids Thermal* **45** 638
[7] De Giorgi M G, Ficarella A, Tarantino M, 2013 *I. J. Heat Fluid Flow* **39** 160
[8] Otsu N, 1975 *Automatica* **11** 23